



**HAL**  
open science

# Statistical Modelling of the Delay Spread of the WBAN channel Considering Room Geometry and Material Characteristics

Badre Youssef, Christophe Roblin

► **To cite this version:**

Badre Youssef, Christophe Roblin. Statistical Modelling of the Delay Spread of the WBAN channel Considering Room Geometry and Material Characteristics. 2023 17th European Conference on Antennas and Propagation (EuCAP), Mar 2023, Florence, Italy. pp.1-5, 10.23919/EuCAP57121.2023.10133637 . hal-04192292

**HAL Id: hal-04192292**

**<https://telecom-paris.hal.science/hal-04192292>**

Submitted on 31 Aug 2023

**HAL** is a multi-disciplinary open access archive for the deposit and dissemination of scientific research documents, whether they are published or not. The documents may come from teaching and research institutions in France or abroad, or from public or private research centers.

L'archive ouverte pluridisciplinaire **HAL**, est destinée au dépôt et à la diffusion de documents scientifiques de niveau recherche, publiés ou non, émanant des établissements d'enseignement et de recherche français ou étrangers, des laboratoires publics ou privés.

# Statistical Modelling of the Delay Spread of the WBAN channel Considering Room Geometry and Material Characteristics

Badre Youssef<sup>1</sup> and Christophe Roblin<sup>1\*</sup>

<sup>1</sup> LTCI, Télécom ParisTech, Institut Mines-Télécom, Paris, France, badre.youssef@telecom-paristech.fr

\* christophe.roblin@telecom-paristech.fr

**Abstract**— This communication presents the development of Delay Spread statistical models of the Wireless Body Area Network indoor channel taking into account parametrically the geometry and the material characteristics of the rooms within the framework of a *scenario-based approach* in the UWB (Ultra Wide Band) context. The study is performed in the 1<sup>st</sup> UWB sub-band  $B = [3.1, 4.8]$  GHz and restricted to the stationary (time-invariant) channel, the subject being motionless. The models are derived from statistical samples obtained thanks to a homemade simplified Ray-Tracing code. The trends of the simulations were compared to the behavior of the Delay Spread of the “classic” indoor channel observed in several experimental studies (for different frequency bands), which confirmed the reliability and consistency of our approach. The models extracted from a set made up of several categories of premises present a very satisfactory goodness of fit for the three considered radio links.

**Index Terms**— Delay Spread, Power Delay Profile, WBAN, indoor propagation, statistical modelling, Statistical Experimental Design.

## I. INTRODUCTION

This article presents statistical models of the Delay Spread (DS)  $\tau_{ds}$  in indoor environment for Wireless Body Area Network (WBAN) communications in the context of the *scenario based approach*, the interest of which is discussed e.g. in [1]. Three Radio Links (RL) are here considered, namely Hip-to-Chest (H2C), Hip-to-Wrist (H2W) and Hip-to-Ear (H2E) and the channel is supposed stationary. The considered frequency band is the first UWB sub-band  $B = [3.1, 4.8]$  GHz (of bandwidth  $\Delta f = 1.7$  GHz).

The DS expression is recalled here for convenience:

$$\tau_{ds}^2 = \frac{\int_0^\infty (\tau - \bar{\tau})^2 p(\tau) d\tau}{\int_0^\infty p(\tau) d\tau} \quad (1)$$

with

$$\bar{\tau} = \frac{\int_0^\infty \tau p(\tau) d\tau}{\int_0^\infty p(\tau) d\tau} \quad (2)$$

and  $p(\tau)$  the Power Delay Profile (PDP), defined as:

$$p(\tau) = \mathbb{E}[|h(\tau)|^2] \quad (3)$$

where  $h$  is the Channel Impulse Response (CIR) and  $\mathbb{E}[\cdot]$  the mathematical expectation. The PDP can be computed from empirical CIRs, directly measured with a channel sounder or obtained from Frequency Domain (FD) measurements – usually with a Vector Network Analyzer (VNA). Nevertheless, the measurement campaigns are time consuming and all the types of premises targeted in the context

of the statistical modelling presented here are generally not available.

However, the statistical modelling of the influence of the indoor environment on the WBAN channel (in a broader context including the DS, but also other key parameters such as the Path Loss), requires relying on samples which are sufficiently representative of their diversity (size and “aspect ratio” of rooms and wall materials). The proposed approach is hence based on: (i) the development of a homemade Ray-Tracing (RT) code, allowing to “sample” easily any type of room, (ii) the use of electromagnetic simulations of antennas worn by a whole body phantom, and (iii) the development of realistic statistical Experimental Designs (ED). They are based on a categorization of environments whose characteristics come from statistical data of the French real estate portfolio (and regulatory standards and recommendations). To our knowledge, the analysis of the influence of the indoor environment on the delay spread with a detailed parametric and statistical modelling in the WBAN context is new.

The methodology and the ED are presented in §II; the §III is devoted to the theoretical approach. Statistical results and DS models are exposed in §IV; Finally conclusions and perspectives are drawn in §V.

## II. METHODOLOGY AND EXPERIMENTAL DESIGN

It is well known that the DS depends on the size of the premises, materials of the walls (reflectivity) and the distance between antennas [2–5]. The latter plays a marginal role for WBANs because the antennas are almost collocated. The objective of the work presented is to finely model the DS according to the size of the rooms, the materials of the walls and the considered RL.

### A. Simplified RT Code

A simplified RT code (based on image theory) considering specular reflections only (up to order 3) has been developed (under Matlab<sup>®</sup>). The simplifying assumptions of the proposed modelling are therefore the following: the rooms are empty and the walls smooth, so that the diffraction on the furniture (and on the irregularities of the walls) and the diffuse scattering are neglected. This tool allows to sample with great flexibility a large number of environments and subject positions (and orientations) within each room. The Channel Transfer Function (CTF)  $H$  is defined here as the

transmission parameter  $S_{21}^{\text{Total}}$  referenced to the input planes of the antennas:

$$H \triangleq S_{21}^{\text{Total}} = S_{21}^{\text{On}} + S_{21}^{\text{Env}} \quad (4)$$

where,  $S_{21}^{\text{On}}$  is the *on-body* contribution (corresponding to the path(s) along, around or close to the body). The environmental contribution  $S_{21}^{\text{Env}}$  is clearly described in [6]. Our code was validated with a proven tool from Beijing Jiaotong University (**Cloud RT**, [7]) and by comparing the data obtained with experimental results [8].

Simulations have been performed in the frequency band  $B = [0.005, 6]$  GHz. The frequency step (5 MHz or 10 MHz) is chosen according to the maximum delay  $\tau_{\text{max}}$  of the Multi Path Components (MPCs), which depends on the size of the rooms and the maximal number of reflections considered  $n_r$  ( $n_r = 3$  here), and of which a good estimate is [10]:

$$\tau_{\text{max}} = \frac{L_d \cdot (n_r + 1)}{c} \quad (5)$$

where  $L_d$  is the large diagonal (i.e. of the parallelepiped).

### B. On Body Contribution

This study deals with three RL: H2C, H2W and H2E as represented in Fig. 1. The choice of the RL was made according to the expected effect of the environment, more or less pronounced depending on the link [9]. The subject, of average build, is modeled by an anthropomorphic inhomogeneous phantom (“*Louis*”) of the IT’IS Foundation Virtual Population suit [11].

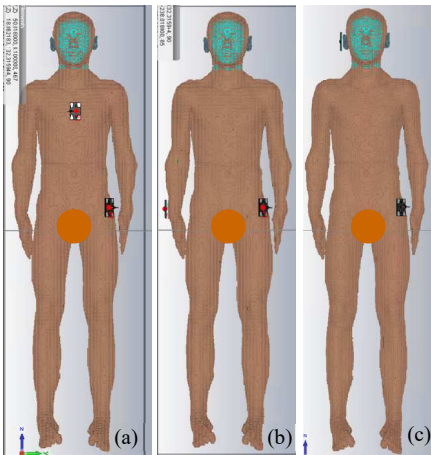


Fig. 1 (a) H2C, (b) H2W and (c) H2E simulated with CST with “*Louis*”.

The on-body clusters ( $S_{21}^{\text{On}}$ ) and the Antenna Transfer Functions (ATF)  $\mathcal{H}^T$  [12] are obtained from Electromagnetic simulations with CST Studio Suite®. These simulations were previously validated by comparison with measurements performed in an anechoic chamber with a homogeneous whole body phantom (“*Kevin*”) whose morphology is close to that of *Louis* [8]. A “homogenized” version of *Louis*, with the same permittivity  $\epsilon_r(f)$  as *Kevin*, was used as an “intermediate model” to compare the simulated and measured radiation patterns. An example of azimuthal cuts of the Mean Realized Gain (defined as  $MRG = \frac{1}{\Delta f} \int_{f_{\text{min}}}^{f_{\text{max}}} \|\mathcal{H}^T(f)\|^2 df$  in [8] and [12]) is shown for the chest and wrist antennas in

Figure 2. The agreement is quite satisfactory in particular in the main lobe.

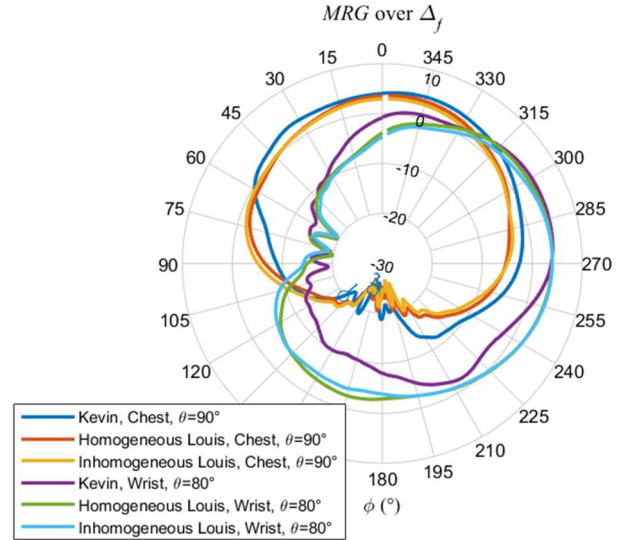


Fig. 2 MRG azimuthal patterns for MSA-BP on Chest and Wrist.

### C. Statistical Experimental Design

One of the peculiarities of WBAN lies in its numerous sources of variability in particular: the subject (movement, posture and morphology [9]), the antennas type and positioning (distance to the body, orientation and polarization), and the environment, notably indoor (dimensions, wall materials, etc.). In this study, only the RL, the environment and the subject location and orientation are variable in the proposed modelling (as inputs parameters of the ED). The others are “fixed”; In particular, the subject (*Louis Inhomogeneous*) is standing still and the antennas used – which are resilient to body proximity effects – are the *Multi-slot Antennas with a Screening Backplane (MSA-BP)* [13], in order to focus specifically on the environmental effects.

#### 1) Environments

Concerning the environments, a categorization was established from a bibliographical search in the specialized literature of real estate according to some criteria: size of the premises, surface “aspect ratio”, wall thickness, etc., [14–16] as well as the wall materials [17–19]. Access to the characteristics of materials ( $\epsilon_r', \epsilon_r'', \sigma$ ) being often fragmented, we also relied on the ITU models [20]. The environments categorization used here is quite similar but simpler than that proposed by the ITU in [21]:

- **Residential:** bedroom, kitchen, bathroom, living rooms,
- **Office:** office, meeting-room, class room, open space,
- **Factory:** industrial and commercial buildings.

In this study, we limited the environments to corridor, office and living room (8 samples for each environment) since simulations for the DS are time consuming given the required small frequency step. From this categorization, the statistical EDs for the parameters considered (dimensions, materials and thicknesses of the walls) were defined quantitatively, by fixing four parameters: the extreme values, the median and the mode (see Table I to Table III). The Beta distribution  $B(\alpha, \beta)$  was chosen for the floor dimensions of the rooms ( $L, W$ )

because its support is bounded and its parameters ( $\alpha$  and  $\beta$ ) can be easily calculated from the parameters of the ED (min, max, median and mode). Moreover, each category being characterized by certain constraints on the aspect ratios of the rooms, the dependencies between  $L$  and  $W$  were quantified by copulas. The statistical samples are obtained by means of the Latin Hypercube Sampling (LHS) technique which is more efficient than the brute force Monte Carlo method [22].

TABLE I. DIMENSIONS STATISTICAL PARAMETERS OF THE CONSIDERED ENVIRONMENTS

Environment	Dimensions (m) [min, max], mode, median		
	L (m)	W (m)	H (m)
Corridor	[1.8, 6], 3.2, 3.5	[0.8, 1.7], 1.1, 1.2	2.4
Office	[4, 6], 4.7, 4.8	[2.2, 3.4], 2.6, 2.7	2.7
Living Room	[5, 10], 6.7, 7.1	[2.8, 4], 3.2, 3.3	2.4

TABLE II. WALLS THICKNESS ACCORDING TO MATERIALS

Wall	Material	Thickness (cm) [min, max], mode, median	
Wall	Bearing wall	Hollow brick	[15, 30], 20, 20
		Reinforced concrete	[20, 35], 23, 25
		Cinder Block	[15, 35], 20, 22
	Bulkhead	Plaster	[15, 30]
		Brick	[5, 15]
	Glass: Single glazing	[0.4, 0.6]	
	Glass: Double glazing	[0.4 1.2 0.4] or [0.4 1.6 0.4]	
Wood (Door)	[3, 4]		
Ceil	Reinforced concrete	[12, 20], 15, 15	
Floor	Reinforced concrete	$L/25$ with a max. of 40 cm	

TABLE III. WALL MATERIALS RELATIVE PERMITTIVITIES

Material	Complex Relative Permittivity [min, max], mode, median	
	Real part	Imag. part
	$\epsilon_r'$	$\epsilon_r''$
Brick	[3, 6], 3.8, 3.8	[0.02, 0.6]
Reinforced concrete	[3, 9], 5.2, 5.8	[0.1, 1.5]
Cinder Block	[2.5, 7], 4, 4.5	[0.1, 1.5]
Plaster	[1.9, 2.9]	0.14
Glass	[4, 7], 6, 6	0.1
Wood	[1.2, 6] 2, 3	0.1

For the reinforced concrete, a conductivity  $\sigma = 0.1$  S/m is also considered.

## 2) Spatial Sampling

Each room is spatially sampled at a medium scale considering different subject locations (*Macro-positions* Mp) and sixteen orientations  $\psi$  (step of  $22.5^\circ$ ) for each Mp. For each  $\psi$ , a spatial sampling at sub-wavelength scale is performed (*micro-position* parameter  $\mu p$ , with  $N_{\mu p} = 6$ ) in order to manage the small scale fading. In our study, the distance between two successive  $\mu p$  is  $d_{\mu p} = \frac{\lambda_{min}}{2} = \frac{c}{2f_{max}} \approx 3$  cm.

To limit the ED size without degrading its statistical representativeness and accuracy, we tried to estimate the

appropriate minimal density of Mp per unit area ( $n_{MP}$  (Mp/m<sup>2</sup>)) with the method explained in [6] using a Kolmogorov-Smirnov test (KS test); for this study  $n_{MP} = 1$  Mp/m<sup>2</sup>. The Mp are sampled with a uniform distribution using the LHS method associated with a maximin algorithm in order to avoid Mp overlapping. The orientations are uniformly distributed (over  $[0, 359]^\circ$ ) and sampled with the LHS method.

## III. THEORETICAL APPROACH

In the literature, different signal processing methods are used to estimate the PDP from the baseband or transposed band of the CTF  $H$ , applying or not a frequency windowing. The choice of the processing used is partly arbitrary (such as that of a specific frequency window) but have a significant impact on the DS value. In order to circumvent arbitrary choices and the associated impacts, we propose to estimate the impulse responses in infinite band  $h^\infty$  with a RT code and some assumptions. It is 1<sup>st</sup> assumed that the plane waves approximation is satisfactory and that the Fresnel coefficients only depend weakly on the frequency, i.e. that the dispersion due to multi-reflections in the walls is small. This is particularly well verified for lossy (thick) walls (see Table III). In Fig. 3 for example, we can observe that the reflection coefficient depends little on the frequency.

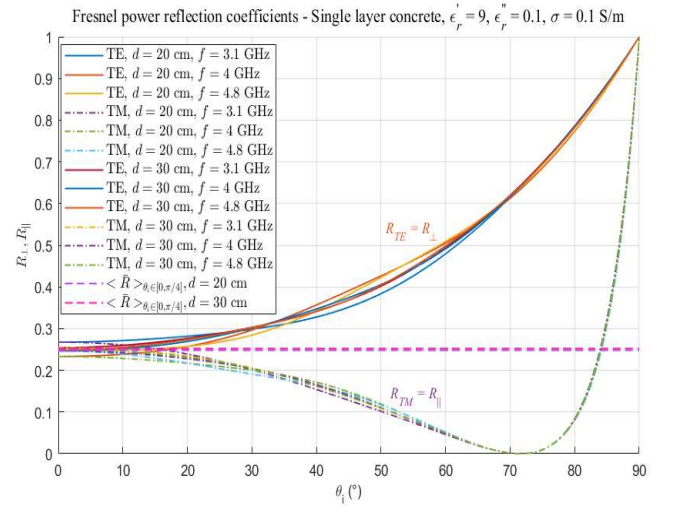


Fig. 3 Fresnel power reflection coefficients - Single layer concrete  $\epsilon_r = 9$ ,  $\epsilon_r'' = 0.1$  and  $\sigma = 0.1$  S/m.

This is even truer if we increase the thickness or  $\epsilon_r''$  (or decrease  $\epsilon_r'$ ).

Second, we neglect the dispersion due to the antennas. This approximation is reasonable because the spread of their Impulse Response (IR) does not exceed a few hundred picoseconds. The infinite band CIR, truncated at maximal delay  $\tau_{nT}$ , reads:

$$h^\infty(t) \sim \hat{h}^\infty(t) \triangleq h_{(nT)}^\infty(t) = \sum_{n=1}^{nT} |a_n| e^{j\xi_n} \cdot \delta(t - \tau_n) \quad (6)$$

where  $|a_n|$  is evaluated (following the above mentioned comments) as the square root of the normalized average power  $P_n^W$  of the path  $n$  as:

$$|a_n|^2 = P_n^W \sim \frac{1}{\Delta f} \int_{f_1}^{f_2} |S_{21}^{(n)}(f)|^2 df \quad (7)$$

This approach avoids the problem of “integrating the side lobes” of the inverse Fourier transform when calculating the DS, but is limited by the abovementioned underlying simplifying assumptions.

Each propagation delay  $\tau_n$  is assessed as the flight time of the path  $n$  (geometrically estimated as  $\frac{r_n}{c}$  with  $r_n$  the path length) to which we add the propagation time in the antennas  $\tau_{ant}$  thus getting back to the reference planes of the measured or simulated  $S_{21}$  parameters. Then the PDP is directly calculated from  $a_n$  and  $\tau_n$  as:

$$PDP(t) = \mathbb{E}[\sum_{n=1}^{n_T} |a_n|^2 \cdot \delta(t - \tau_n)] \quad (8)$$

Under the above mentioned assumptions (1) becomes:

$$\tau_{ds}^2 = \frac{\sum_{n=1}^{n_T} |a_n|^2 (\tau_n - \bar{\tau})^2}{\sum_{n=1}^{n_T} |a_n|^2} \quad (9)$$

with

$$\bar{\tau} = \frac{\sum_{n=1}^{n_T} |a_n|^2 \tau_n}{\sum_{n=1}^{n_T} |a_n|^2} \quad (10)$$

The limitations of the proposed approach are that it does not take into account the diffraction and more generally the dense component of the channel (DMC): the rooms are empty and the roughness and irregularities of the walls are not taken into account so that the diffuse component is neglected, and the number of specular reflections is limited to 3. However, the main objective here is to identify the main trends of the DS in relation to the characteristics of the environment.

#### IV. RESULTS AND DELAY SPREAD MODELLING

The input parameter  $\Lambda$  for our DS model is based on two environment characteristics: the geometry and the materials. The latter are characterized by  $\bar{R}_{av}$ , the mean of the square modulus of the multi-reflection Fresnel coefficients  $\bar{R}_{TE}$  and  $\bar{R}_{TM}$ , i.e.:

$$\bar{R}_{av} = \frac{1}{2} \langle \bar{R}_{TE}^2 + \bar{R}_{TM}^2 \rangle_{\theta_i, Wall} \quad (11)$$

For each environment,  $\bar{R}_{av}$  is averaged over the operational band  $\Delta f$ , the four vertical walls, and a range of angles of incidence  $\Delta \theta_i = 45^\circ$  ( $\theta_i \in [0, 45]^\circ$ ). The latter actually depends on the RL, but for almost all of them  $\Delta \theta_i \leq 45^\circ$  typically, except when the subject is very close to a wall (for RL which are not considered here, e.g. “Hip-to-Toes”).

According to Hansen’s approach exposed in [3] (eq. (7) & (8)), the DS can be expressed as:

$$\tau_{DS} \sim \frac{L}{c(1+\alpha_{AR})} \cdot \frac{1}{\ln \frac{1}{\bar{R}_{av}}} \cdot \frac{1}{1 - \frac{c \tau_{max} (1+\alpha_{AR})^2}{12L} \ln \frac{1}{\bar{R}_{av}}} \quad (12)$$

where  $\alpha_{AR} = \frac{3}{\sqrt{1+\kappa^2+\chi^2}}$  is a room “aspect ratio” coefficient and  $\kappa = \frac{W}{L}$ ,  $\chi = \frac{H}{L}$ , with  $L$ ,  $W$  and  $H$  the length, width and height of rooms. Note that the calculation of  $\bar{R}_{av}$  differs from that of [3].

This approach guided us in the search for a simple model structure integrating the geometry of the rooms (similar to the experimental approaches of [2] and [4]), as well as the material characteristics of the walls. Since the subject's

orientation in the environment ( $\psi$ ) is assumed to be completely random, Hansen’s model, while remaining restricted to omni-directional antennas, is still roughly valid if the CTF is statistically averaged over this parameter, which is what we do here (over 16 random  $\psi$  values for each Mp) just as it is averaged over frequency and small spatial scale. The structure of the proposed *single-parameter* linear model is therefore:

$$\tau_{DS}(RL, \bar{R}_{av}, L, \alpha_{AR}) = \tau_{DS}^{(0)}(RL) + \alpha(RL)\Lambda + \delta\tau_{DS}(RL) \quad (13)$$

where  $\Lambda = \frac{L}{(1+\alpha_{AR}) \ln \frac{1}{\bar{R}_{av}}}$  and where the “residuals” (i.e. the model error) are considered as a random variable which is found to follow a zero-mean normal distribution  $\mathcal{N}(0, \sigma_{\tau_{DS}}^2)$  of variance  $\sigma_{\tau_{DS}}^2$ . The parameters of the models and the coefficient of determination  $R^2$  obtained for each RL are presented in Tables IV and V. The “goodness of fit” given by  $R^2$  is very satisfactory for each RL.

TABLE IV. LINEAR REGRESSION MODEL PARAMETERS

RL	$\alpha$	$\tau_{DS}^{(0)}$ (ns)	$\sigma_{\tau_{DS}}$ (ns)
H2C	12.1	-3.4	1.2
H2W	8.5	2.7	0.9
H2E	7	2.3	1

TABLE V. MODELS  $R^2$  FOR EACH RL

RL	H2C	H2W	H2E
$R^2$	0.93	0.92	0.86

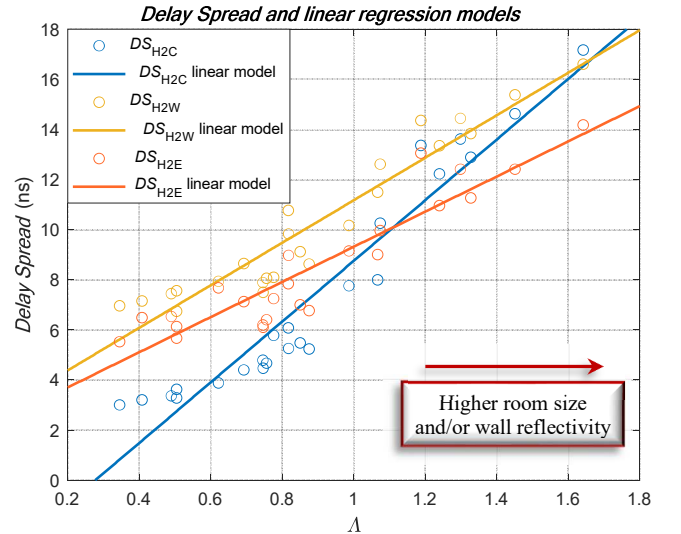


Fig. 4 Mean DS representations as a function of  $\Lambda$  for each RL.

Another simpler approach is to adopt as an explanatory parameter  $\Lambda' = \bar{R}_{av} \sqrt{A_{Floor}}$ , where  $A_{Floor}$  is the floor area, as has been observed in several experimental works including [2]. For each RL, a DS model has been extracted by linear regression, as:

$$\tau_{DS}(RL, \bar{R}_{av}, A_{Floor}^{1/2}) = \tau_{DS}^{(0)'}(RL) + \alpha'(RL) \cdot \Lambda' + \delta'_{\tau_{DS}}(RL) \quad (14)$$

in which  $\alpha'$  and  $\tau_{DS}^{(0)'}$  are the model parameters,  $\delta'_{\tau_{DS}}$  is the model error following a zero-mean normal distribution  $\mathcal{N}(0, \sigma_{\tau_{DS}}'^2)$  of variance  $\sigma_{\tau_{DS}}'^2$ . For this parameter the coefficient of determination  $R^2$  remain quite satisfactory for each RL ( $R_{H2C}^2 = 0.87$ ,  $R_{H2W}^2 = 0.85$  and  $R_{H2E}^2 = 0.77$ ). The moderate degradation observed is explained by the lack of consideration of the room aspect ratio  $\alpha_{AR}$ .

## V. CONCLUSIONS AND PERSPECTIVE

The reliability and consistency of our approach have been confirmed by comparing the trends obtained with simulations to the behavior of the Delay Spread of the “classic” indoor channel observed in several experimental studies (for different frequency bands). This confirms also that the simplifying assumptions chosen are well suited to our use context.

The simulation approach also enables to have samples that are both qualitatively and quantitatively more representative than what is possible to reach experimentally. In addition to being satisfactory, the proposed models are new to our knowledge, notably in the WBAN context (where the antennas are almost co-located). Moreover, the models are also better founded in terms of the physics of the phenomena involved, and more detailed in terms of the explanatory parameters used, than experimental work such as that published for example in [2].

Finally, in the context of a related work, notably concerning the modeling of the PL, we have established a more complete categorization of environments (including about fifteen categories) than the one used here. The corresponding experimental designs are already established and can be used for a delay spread modeling to be extended to more environments. Similarly, the limited number of interactions (3 specular reflections here) can be increased to strengthen the relevance of the results obtained. Finally, the approach will be extended to other radio links (17 RL are already usable in the RT code). In both cases, the only limitation is the significant computational cost.

## REFERENCES

[1] C. Roblin et al, “Antenna design and channel modelling in the BAN context — part II: channel,” *Annals of telecommunications* (Springer), vol. 66, no. 3/4, March/April 2011, pp. 157–175.  
[2] J. T. E. McDonnell, TimP. Spiller, Tim A. Wilkinson, “Characterization of the Spatial Distribution of RMS Delay Spread in Indoor LOS Wireless Environments at 5.2GHz,” *Personal Systems Laboratory HP*, Sept. 1998.  
[3] J. Hansen, “Analytical Calculation of Power Delay Profile and Delay Spread with Experimental Verification,” *IEEE Communications Letters*, vol.7, no. 6, June 2003, pp. 257 - 259.  
[4] A. Kajiwara, “Effects of polarization antenna directivity and room size on DS in LOS indoor radio channel,” *IEEE Transactions on Vehicular Technology*, vol. 46, no. 1, Feb. 1997, pp. 169-175.  
[5] M. Drozdowska, A. Al-Jzari, “RMS Delay Spread Model for 60 GHz Band for Offices and Conference Rooms,” in *Proc. 16th Eur. Conf. on Antennas and Propagation (EuCAP)*, Madrid, Spain, Mar. 27–Apr. 01, 2022.  
[6] B. Youssef and C. Roblin, “Statistical Modelling of WBAN channels in Indoor Environments Based on Measurements and Ray Tracing,” in *Proc. 15th Eur. Conf. on Antennas and Propagation (EuCAP)*, Düsseldorf, Mar. 22–26, 2021.  
[7] D. He, B. Ai, K. Guan, L. Wang, Z. Zhong and T. Kürner, “The Design and Applications of High-Performance Raytracing Simulation Platform for

5G and Beyond Wireless Communications: A Tutorial,” *IEEE Communications Surveys & Tutorials*, vol. 21, no. 1, first quarter 2019.  
[8] B. Youssef and C. Roblin, “A Statistical Model for On-Body Channels in Indoor Considering Rooms Geometry and Subject Location,” *2019 13th Eucap, Krakow, Poland*.  
[9] B. Youssef and C. Roblin, “A Statistical Assessment of Anthropomorphic Characteristics Impacts on WBAN Communications,” in *Proc. 16th Eur. Conf. on Antennas and Propagation (EuCAP)*, Madrid, Mar. 27–Apr. 01, 2022.  
[10] T. Huschka, “Ray Tracing Models for Indoor Environments and their Computational Complexity,” *PIMRC*, 1994.  
[11] IT’IS Foundation Virtual Population, <https://itis.swiss/virtual-population/>.  
[12] C. Roblin, “Ultra Compressed Parametric Modelling of UWB Antenna Measurements,” in *Proc. 1st Eur. Conf. on Antennas and Propagation (EuCAP)*, Nice, Nov. 6–10, 2006.  
[13] Y.-F. Wei and C. Roblin, “Multislot Antenna with a Screening Backplane for UWB WBAN,” *Int. J. of Ant. And Propag. (IJAP)*, Hindawi Publishing Corporation, vol. 2012.  
[14][https://fr.wikipedia.org/wiki/Code\\_de\\_la\\_construction\\_et\\_de\\_l%27habitation](https://fr.wikipedia.org/wiki/Code_de_la_construction_et_de_l%27habitation)  
[15] [https://fr.wikipedia.org/wiki/Taille\\_des\\_logements\\_en\\_France](https://fr.wikipedia.org/wiki/Taille_des_logements_en_France)  
[16] AFNOR Recommendations [https://infosdroits.fr/wp-content/uploads/2012/11/AFNOR-35\\_102.pdf](https://infosdroits.fr/wp-content/uploads/2012/11/AFNOR-35_102.pdf)  
[17] F. Sagnard, “Caractérisation de matériaux en ULB,” *Ecole d’automne ULB - GDR Ondes*, Valence, Oct. 23–27, 2006.  
[18] R. Wilson, “Propagation Losses Through Common Building Materials 2.4 GHz vs 5 GHz,” “Reflection and Transmission Losses Through Common Building Materials,” *Magis Network Inc*, 2002.  
[19] M. Lott, I. Forkel, “A Multi-Wall-and-Floor Model for Indoor Radio Propagation,” *IEEE VTS 53rd Vehicular Technology Conf.*, Spring 2001.  
[20] ITU-R P.2040-2, “Effects of building materials and structures on radiowave propagation above about 100 MHz,” 09/2021.  
[21] ITU-R P.1238-8, “Propagation data and prediction methods for the planning of indoor radiocommunication systems and radio local area networks in the frequency range 300 MHz to 100 GHz,” 07/2015.  
[22] M. D. McKay, R. J. Beckman, and W. J. Conover, “A comparison of three methods for selecting values,” *Technometrics*, vol. 21, no. 2, 05/1979.